ELSEVIER

2005 Special issue

Firing rate modulation: A simple statistical view of memory trace reactivation

Francesco P. Battaglia [a,*], Gary R. Sutherland [b], Stephen L. Cowen [b], Bruce L. Mc Naughton [b], Kenneth D. Harris [c]

[a] *Laboratoire de Physiologie de la Perception et de l'Action, CNRS-Collège de France, Paris Cedex 05, France*
[b] *Arizona Research Laboratories Division of Neural Systems, Memory and Aging, University of Arizona, Tucson, AZ, USA*
[c] *Center for Molecular and Behavioral Neuroscience, Rutgers, The State University of New Jersey, Newark, NJ, USA*

Abstract

Memory trace reactivation in hippocampal ensembles during sleep has been suggested as a coordinating mechanism for consolidation of new memories. Here we propose a simple statistical scheme allowing analysis of the reactivation of firing rate modulations, with a well-defined null hypothesis. This method allowed reliable detection of ensemble reactivation across three experimental settings. Reactivation of firing rate modulations mirrors several properties of commonly studied reactivation measures: it is stronger during hippocampal sharp waves, and decays over a period of 10–20 min.

Moreover, in some conditions, firing rate reactivation covaries with reactivation of cell pair cross-correlations, suggesting the two phenomena reflect similar processes. We propose an attractor network model, with pre-wired attractors, in which experience selects and primes some attractors. Priming occurs by either experience dependent synaptic plasticity or changes in neuronal excitability. Primed attractors are more likely to activate in the following sleep, inducing reactivation of both rates and cross-correlations.
© 2005 Published by Elsevier Ltd.

1. Introduction

Although memories may be formed of single-trial, unique events, it is widely held that the physical changes underlying permanent memory formation continue for some time after the event being remembered. In particular, it has been hypothesized that a 'memory consolidation' process, occurring in sleep after a learning experience, is essential for formation of permanent memory traces in the brain (Buzsaki, 1989; Marr, 1970, 1971; McNaughton, Barnes, Battaglia, Bower, Cowen and Ekstrom, 2003).

Lesion data have demonstrated the implication of the hippocampus and the medial temporal lobe in new memory formation in humans and rats (Broadbent, Squire, & Clark, 2004; Moser, Moser, & Andersen, 1993). While the hippocampus is crucial for acquisition of new memories and for the retention of recently formed memories, its importance decreases for memories acquired at more remote

times; the final storage of those memories may take place elsewhere, and may be guided by information provided by the hippocampus during offline periods. In fact, hippocampal offline activity across many weeks after memory acquisition is necessary for retention (Riedel, Micheau, Lam, Roloff, Martin and Bridge, 1999). It has therefore been suggested that memory consolidation requires that hippocampal neural assemblies activated during learning be reactivated during subsequent sleep, as has been demonstrated in a variety of experimental settings and with different statistical techniques (for a review see Sutherland and McNaughton, 2000). Although some insights into the possible mechanisms of reactivation, such as its NMDA receptor dependence (Stanis et al., 2004) have been shown, the detailed mechanism of reactivation still remains to be elucidated; nevertheless, answers to many specific questions may now be coming within reach, thanks to the unprecedented possibility of simultaneous recording from ensembles of many neurons (Buzsaki, 2004; Wilson and McNaughton, 1993). In particular, does memory consolidation require activation of precise patterns of activity (Lee and Wilson, 2002; Skaggs and McNaughton, 1996; Wilson and McNaughton, 1994), or merely increased firing rates of appropriate neurons (Zhang

---

List of mathematical symbols

α	strength of the experience-dependent synaptic potentiation (in the model)
β	strength of the experience-dependent change in excitability (in the model)
$f^i_{S1,M,S2}$	firing rate for the ith cell during, respectively, the *sleep 1*, *maze*, *sleep 2* epochs
h_i	neural input field (in the model)
G	gain of the threshold-linear neural response function
H_i	external input to ith cell during sleep (in the model)
I	rate of the global inhibitory unit (in the model)
J_{ij}	value of the synaptic connection between the ith and the jth cell (in the model)
r_{MS1}, r_{MS2}, r_{S1S2}	correlation between the zero-lag cell-pair correlation matrices observed, respectively, in *maze* and *sleep 1*, *maze* and *sleep 2*, *sleep 1* and *sleep 2*
τ	time constant for the Wilson-Cowan neural dynamics (in the model)
ξ^μ_i	value of the μth pre-wired pattern on the ith cell (in the model)
θ	threshold of neural response function (in the model)
V_i	firing rate for the ith cell (in the model)
X^i_0	baseline log-firing rate for the ith cell
X^i_S	sleep baseline log-firing rate for the ith cell
$X^i_{S1,M,S2}$	log-firing rate modulations specific to the *sleep 1*, *maze*, *sleep 2* epochs

---

and Linden, 2003)? Does consolidation require the repetition of precise temporal sequences of cell firing that occurred in previous behavior? Does memory consolidation occur preferentially during particular points of the sleep cycle, or during particular population events such as hippocampal sharp-waves (Kudrimoti, Barnes, & McNaughton, 1999)?

Distinguishing between these particular alternatives will require not only carefully controlled experiments, but also careful statistical analyses. First, these biological conjectures must be turned into precise null hypotheses regarding the structure of population spike trains and field potentials. Second, statistical methods must be developed that can test these hypotheses, without making unjustified assumptions concerning the statistical distribution of the data. Finally, these methods must be robust against possible artifacts such as misidentification of extracellularly recorded neurons. In this paper, we seek to develop a statistically rigorous methodology to investigate the simplest possibility; that of reactivation of firing rate modulations. We test this hypothesis using a novel, conservative cross-validation approach, in which model misspecification is likely to yield type II rather than type I errors. We find that the activation of neurons in the initial phases of sleep is correlated with the degree of activity during recent waking behavior.

We then discuss the relationship between the reactivation of firing rate modulations and the effects observed on quantities that seem to describe more directly ensemble activity, such as cell-pair correlations, then we discuss a simple theoretical model delineating a possible scenario in which reactivation of firing rate modulation and cross-correlation originate from the same network effects.

2. Experimental methods

2.1. Animal subjects, surgical and recording techniques

Male Fisher 344 or Brown Norway/F344 hybrid rats were used for these experiments. All procedures were conducted according to approved University of Arizona Institutional Animal Care and Use Committee protocols and NIH standards. The rats were implanted, under pentobarbital or isofluorane anesthesia, with a circular array of 14 separately moveable microdrives ('HyperDrive'), each one guiding a tetrode in the dorsal CA 1 region of the hippocampus. During recording, the tetrode signal was filtered between 600 Hz and 6 kHz, and spike waveforms were acquired at 32 kHz each time the signal exceeded a manually set threshold. Spike waveforms were sorted offline by means of a semi-automatic clustering algorithm (BBClust, author: P. Lipa), and the classification was refined manually using custom-written software (MClust, author: A.D. Redish). The recording device and the parallel recording technique have been described in detail elsewhere (Battaglia, Sutherland, & McNaughton, 2004; Gothard, Skaggs, Moore, & McNaughton, 1996; Wilson and McNaughton, 1993). Putative pyramidal cells and interneurons were discriminated by considering the average firing rate, cell burstiness and spike waveform. Only pyramidal cells were analyzed in this work. The signal from tetrodes placed in the CA1 pyramidal layer was also filtered between 100 and 300 Hz and a thresholding algorithm was used to detect the ripple oscillations that occur during sharp wave events.

2.2. Behavior

Experiment A was described by Battaglia et al. (2004) as Experiment C. Briefly, before surgery the rat was trained to shuttle back and forth on a linear track in an environment different from those used for the recordings, with food reward at the two ends. For the experiments, two structurally identical linear tracks (180×8 cm), placed in two adjacent recording environments, were used. One track ('cue-rich' track) was enriched with local cues including steel wool, cotton, odors (vanilla essence), various kinds of hurdles that the rats were required to climb over, or which limited the accessible width of the track. The other ('cue-poor') was left unadorned. In recording sessions, the rats were allowed to rest in a towel-lined flower pot placed next to the track for 20–25 min (*sleep 1*

epoch), then they performed the shuttling task on one of the tracks (alternating the two in consecutive experimental sessions) for 15 min (*maze 1* epoch), and then rested again in the flowerpot for another 20–25 min (*sleep 2* epoch). Afterwards, the rat was moved to the other environment for a shuttling session on the other track (*maze 2* epoch) and then allowed to rest in a flower pot for another 20–25 min (*sleep 3* epoch). Because of the difficulties involved in comparing recordings from two data acquisition setups, only the *sleep 1/maze 1/sleep 2* epoch were considered for this analysis. Note also that the designation of epochs as 'sleep' periods is by convention only. The animals rested quietly and were often in apparent slow-wave sleep, but at some times they were in a quiescent waking state. The latter is a sufficient condition for memory trace reactivation (Kudrimoti et al., 1999).

In Experiment B, described by Battaglia et al. (2004) as Experiment A, the rats shuttled back and forth on a 'cue-rich' circular track, with different portions covered with materials of different textures, and other kind of local visual, olfactory, and tactile cues. Experimental sessions followed a *sleep 1/maze/sleep 2* protocol, with sleep periods of 20–25 min.

In Experiment C (Karten et al., 2002), the rats shuttled on a T-maze between the base arm and one of the two collinear arms (alternating the two between trials). Food reward was delivered at all three arm ends, on a probabilistic schedule: the base arm was rewarded in 50% of the trials, the two collinear arms were rewarded, respectively, 20 and 80% of the times. Each

experimental day, two running sessions were recorded, in two maze configurations: in one, the rat had access to the full arm extent, in the second, the arms were shortened with barriers. The sessions were preceded, interspersed, and followed by sleep sessions of 20–25 min (*sleep 1/maze 1/sleep 2/maze 2/sleep 3* protocol). Reactivation analyses are performed considering

1. the effect of maze 1 activity on the subsequent sleep period (sleep 2), using the preceding sleep period (sleep 1) as control
2. the effect of maze 2 activity on the subsequent sleep period (sleep 3), using the preceding sleep period (sleep 2) as control

For most analyses only the last 10 min of the preceding sleep period and the first 10 min of the following sleep period were used. Since, *sleep 2* lasted for at least 20 min, non-overlapping portions of that epoch were used when examining the effects of the *maze 1* epoch and of the *maze 2* epoch.

2.3. Analysis methods

Firing rates of principal cells in the hippocampus have widespread and skewed distributions (Fig. 1). A log-transformation was, therefore, applied to make the distribution closer to Gaussian, allowing the use of linear analyses.
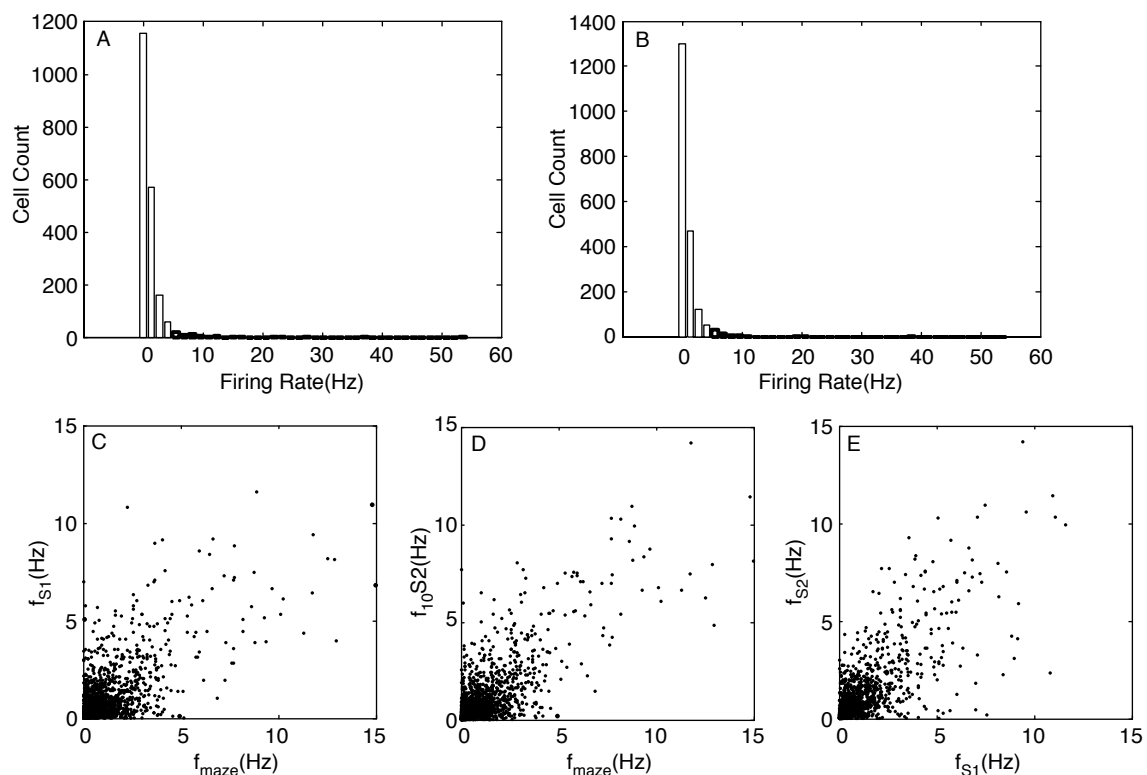

Fig. 1. Distribution of epoch-averaged population firing rates. A. Histogram of population firing rates averaged over the *maze* epoch. B. Histogram of population firing rates averaged over the *sleep 1* epoch. C–E. Scattergrams of the population firing rates. C. *X*-axis: average firing rates for all cells during the *maze* epoch. *Y*-axis: average firing rates during the *sleep 1* epoch. D. *X*-axis: average firing rates during the *maze* epoch. *Y*-axis: average firing rates during the *sleep 2* epoch. E. *X*-axis: average firing rates during the *sleep 1* epoch. *Y*-axis: average firing rates during the *sleep 2* epoch.

We consider the firing rates in sleep immediately before the behavioral task (the *sleep 1* epoch, S1), during behavior (the *maze* epoch, M), and sleep immediately after (*sleep 2* epoch, S2). In a reactivation analysis, we seek to investigate whether neurons which fire at elevated rates during M continue to fire at elevated rates during S2. The widespread variability in baseline rates complicates this analysis. The S1 epoch is used to provide information about each cell's baseline firing rate, when studying the correlation between M and S2.

In a complex analysis, it is essential to formalize precisely the null hypothesis being tested. The null hypothesis here is that there are no correlations between the activity in *maze* and *sleep 2*, other than resulting from variable baseline activity. More precisely, the firing rates of the *i*-th cell in the three epochs are modeled by

$$\log(f^i_{S1}) = X^i_0 + X^i_S + X^i_{S1}$$
$$\log(f^i_M) = X^i_0 + X^i_M$$
$$\log(f^i_{S2}) = X^i_0 + X^i_S + X^i_{S2}$$

Here, X^i_0 represents the baseline firing rate of cell i, X^i_S characterizes the relative preference of this neuron for firing during sleep as compared to waking, and X^i_{S1}, X^i_{S2} and X^i_M represent the session-specific firing rate modulations of neuron i in the three epochs. The null hypothesis is that the X's are independent Gaussian variables, and that all correlation between rates therefore arises due to common influence of the baseline variables X^i_S and X^i_0. In particular, we aim to test the hypothesis that X^i_{S2} and X^i_M are uncorrelated.

An initial approach might be to consider the correlation between $\log(f^i_M/f^i_{S1})$ and $\log(f^i_{S2}/f^i_{S1})$. In these variables, the effect of the baseline X^i_0 is subtracted away. However, the subtracted values both still contain X^i_{S1}, and a spurious correlation will, therefore, be observed. This problem is alleviated by dividing the Sleep 1 session into two halves, S1a and S1b. We then examine the correlation of $X_{S2S1} = \log(f_{S2}/f_{S1a}) = X_2 - X_{1a}$ with $X_{MS1} = \log(f_M/f_{S1b}) = X_M - X_S - X_{1b}$. This provides a test of the null hypothesis, provided that X_{1a} and X_{1b} are uncorrelated. This latter assumption may be validated by considering the return to baseline of the population vector autocorrelogram during sleep (Fig. 3).

As a further control, we also examine the reverse analysis or 'preactivation', in which the same formula is used, swapping the roles of *sleep 1* and *sleep 2* (Pennartz, Lee, Verheul, Lipa, Barnes and McNaughton, 2004).

The cell-pair correlation reactivation was computed as described by Kudrimoti et al. (1999) and by Hoffman and McNaughton (2002). For each epoch, spike trains were binned into T intervals of 100 ms, producing sequences of spike counts $f_i(t)$. The normalized correlation C between each pair (ij) of spike trains was computed using the equation:

$$C_{ij} = \frac{1/T \sum_{t=1}^{T} f_i(t)f_j(t) - 1/T^2 \sum_{t=1}^{T} f_i(t) \sum_{t=1}^{T} f_j(t)}{\sqrt{1/T^2 \sum_{t=1}^{T} f_i^2(t) \sum_{t=1}^{T} f_j^2(t)}}.$$

The explained variance (EV) of correlations from *sleep 2* and *maze*, given the correlations of *sleep 1* was then computed. The EV was calculated based on the square of the partial correlation coefficients:

$$EV = r^2_{MS2|S1} = \left(\frac{r_{MS2} - r_{MS1}r_{S2S1}}{\sqrt{\left(1 - r^2_{MS1}\right)\left(1 - r^2_{S2S1}\right)}} \right)^2,$$

where r_{AB} indicates the Pearson correlation coefficient between the cell pair correlations C_{ij} computed in epoch A and in epoch B.

2.4. Simulation methods

Spontaneous activity during sleep was simulated in a recurrent network of $N = 2000$ threshold-linear neurons. The simulation is a refinement and extension of the model published previously by Shen and McNaughton (1996).

The time course of the input-field variables h_i, modeling the total input received by each neurons was dictated by the (Wilson and Cowan, 1972) equations

$$\tau \frac{d}{dt} h_i = -h_i + \sum_{j \neq i} J_{ij} V_j + I + H_i$$

(Rolls and Treves, 1998; Treves, 1990), where J_{ij} is the matrix of the synaptic connections, I is an inhibition term, uniform across neurons, that prevented the total network activity from exceeding a fixed limit. H_i is an external input term. The time constant τ is not ascribed here any precise biological meaning, and was adjusted in order to moderate spurious dynamical phenomena related to synchronous unit update (Amit, 1989) such as 2-cycles. Only the stable states reached by the dynamics are of interest here. The activations V_i, representative of firing rate variables for each neuron were related to the input field by a threshold linear function:

$$V_i = G(h_i - \theta),$$

with gain $G > 1$ and threshold θ.

The synaptic matrix J_{ij} encoded $p = 100$ (0, 1) random patterns ξ^μ according to the Hopfield-like formula:

$$J_{ij} = M \sum_\mu \xi^\mu_i \xi^\mu_j,$$

where M is a normalization factor.

This synaptic encoding is assumed to be already in existence at the beginning of the *maze* epoch, and to influence the activity during the maze: in this simplified scenario, the Hopfield-like matrix plays the same role that it has been advocated for a topology-embedding, 'multi-chart' synaptic architecture (Redish and Touretzky, 1998; Samsonovich and McNaughton,

1997). Roughly, each attractor then represents a possible representation of a physical location. In any single environment, only a relatively small fraction (15–25%) of hippocampal cells have a place field. In our modeling framework, this is equivalent to saying that only a few of the pre-wired attractors are actually activated during the maze experience. For simplicity, we assumed here that only one of the attractors was active during the *maze* epoch.

As suggested by Shen and McNaughton (1996), two hypotheses were considered about how a trace of the maze activity could be encoded in the network. First, a LTP-like change in synaptic strength, potentiating the synapses between units that were co-active during the *maze* epoch (that is, in the *l*-th pattern):

$$J'_{ij} = J_{ij} + \sum_{\mu} \alpha M \xi_i^l \xi_j^l,$$

where α represent the strength of the synaptic potentiation.

Second, a change in cellular excitability proportional to a given cell's activity in the *maze* epoch (dictated by the *l*-th pattern) was considered, in the form of a leftward shift in the activation function threshold:

$$\theta'_i = (1 - \beta \xi_i^l) \theta$$

where β represents the intensity of the facilitation.

Spontaneous activity during sleep was modeled by injecting into each cell a constant, positive, exponentially distributed noise term H_i. The network dynamics was allowed to relax, and the process was repeated with 500 realizations of the noise. Only the steady state configurations, that is, the configurations obtained at the end of the relaxation process, were retained for analysis.

3. Results

3.1. Summary of results

We characterized memory trace reactivation in cell ensembles, by means of a measure of the correlation between the global firing rates in the *maze* epoch and in the subsequent sleep. The measure was designed to eliminate the spurious correlations induced by the distribution of the baseline firing rate across a population of hippocampal pyramidal cells, using data recorded in a sleep epoch before the maze session to assess the baseline, in a cross-validation scheme. Reactivation was observed in a large majority of the experimental sessions considered. Also, similarly to cell-pair correlation measures of reactivation, reactivation was stronger during sharp waves than in inter-sharp wave periods, and showed a declining time course across the first 20 min of the sleep session. We also find that rate and cell-pair correlation measures of reactivation are correlated, at least in some experimental conditions. We provide a simple scenario, in an attractor network with attractors pre-wired in the connectivity matrix, where reactivation of both firing rate modulations and cell-pair correlations are observed as an effect of experience related

changes in either the synaptic structure or the intrinsic excitability, causing a shift in the proportion of time each of the pre-existent attractors is reached in spontaneous activity.

3.2. Analyzed data

A total of 2035 putative pyramidal cells were recorded from eight rats: 507 cells from two rats, 19 datasets for Experiment A, 514 cells from two rats, 16 datasets for Experiment B, 1014 cells from four rats, 27 datasets, in Experiment C.

3.3. Distributions of firing rates and log-firing rates

The population distribution of firing rates is very skewed and very far from Gaussian both while running on the track (mean = 1.1 Hz, SD = 2.38 Hz; skewness = 10.2; kurtosis = 169.5; Fig. 1A) and during sleep (mean = 0.98 Hz, SD = 1.96 Hz; skewness = 9.06; kurtosis = 140.9; Fig. 1B). This is expected, given the large number of pyramidal cells with very low firing rates (in both cases the mode of the distribution was very close to 0). When comparing the average firing rates across epochs, a relatively strong correlation is observed (maze vs. pre-sleep: $r^2 = 0.44$ Fig. 1C, maze vs. post-sleep: $r^2 = 0.53$ Fig. 1D, pre-sleep vs. post-sleep: $r^2 = 0.53$ Fig. 1E). The correlation is mostly generated by a minority of high firing rate cells, and seems to be dominated by the wide range of intrinsic excitability of the cells. Thus, using correlations between average firing rates as a measure of the similarity between the population patterns of cell excitability in different epochs misses the structure contained in the activity of the low firing rate hippocampal pyramidal cells, which contain a great deal of spatial information, and are an important component of the hippocampal activity pattern.

A better choice to compare the population activities between different epochs may be to take the logarithm average firing rates. Log-firing rates have a distribution closer to normal in both the *maze* and *sleep* epochs (maze: mean = −0.28, SD = 0.65; skewness = − 0.8; kurtosis = 4.23; Fig. 2A, sleep: mean = −0.34, SD = 0.59; skewness − 0.20, kurtosis = 3.19; Fig. 2B). The slightly higher skewness of the *maze* distribution mirrors the fact that, during self-motion, hippocampal pyramidal neurons with a place field on the track are very active, whereas cells without a place field are nearly silent. The population patterns of log-firing rates are less correlated between different epochs than was the case for firing rates (maze vs. pre-sleep: $r^2 = 0.056$ Fig. 2C, maze vs. post-sleep: $r^2 = 0.12$ Fig. 2D, pre-sleep vs. post-sleep: $r^2 = 0.21$ Fig. 2E). The scatter plots in Fig. 2C–E show that the weight of high firing rate cells in the correlation is reduced, and reveal an absence of between-epoch correlations for low firing rate cells.

3.4. Firing rate patterns decorrelate in time

The assumption in the cross-validation scheme used here is that firing rates in the first and last 10 min of the pre-sleep epoch do not contain correlations besides the baseline correlation due to the variability across cells in intrinsic
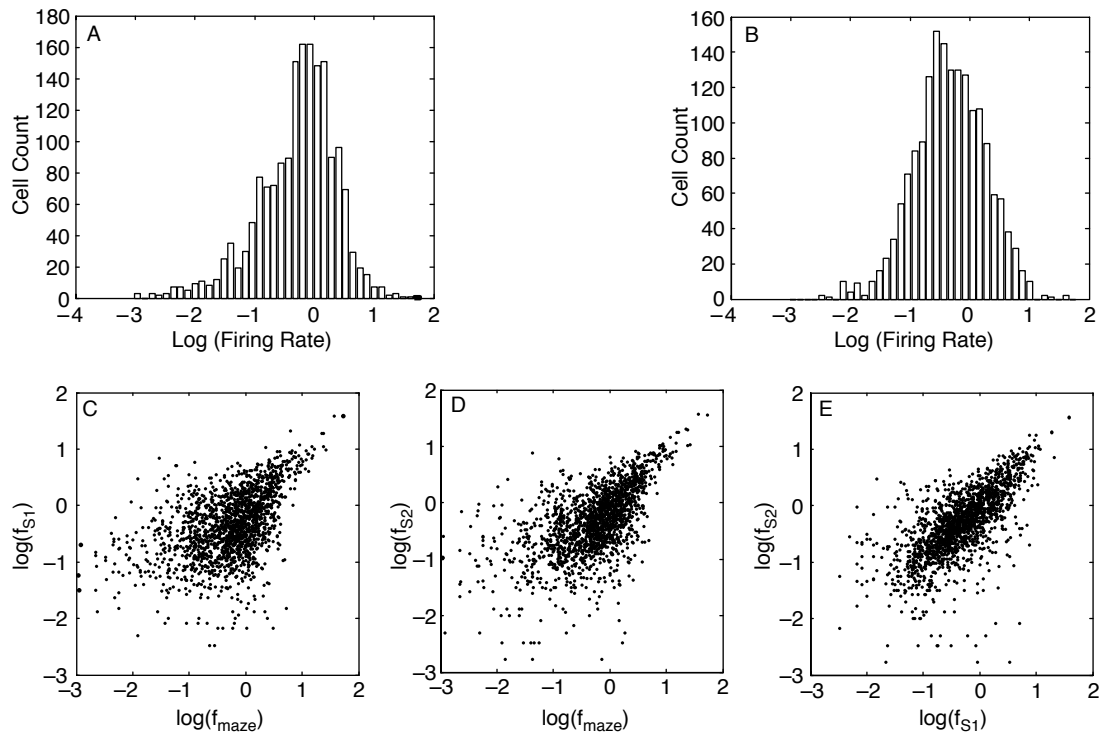
Fig. 2. Distribution of the logarithm of epoch-averaged population firing rates (*log-firing rates*). A. Histogram of population log-firing rates during the *maze* epoch. B. Histogram of population log-firing rates during the *sleep 1* epoch. C–E. Scattergrams of the population log-firing rates. C. X-axis: average log-firing rates for all cells during the *maze* epoch. Y-axis average log-firing rates during the *sleep 1* epoch. D. X-axis: average log-firing rates during the *maze* epoch. Y-axis: average log-firing rates during the *sleep 2* epoch. E. X-axis: average log-firing rates during the *sleep 1* epoch. Y-axis: average log-firing rates during the *sleep 2* epoch.

excitability. This means that any transient correlation in the firing rates would have to decay in a time shorter than 10 min. To test this, firing rates were calculated for 1 min time bins. The correlations were computed between the obtained population vectors. The average correlation for time bins at a lag t is shown in Fig. 3. In fact, correlation decays to about 0.85 in 10 min, still remaining at values higher than the correlations observed between *sleep 1* and *sleep 2* for time lags comparable with the duration of the sleep epochs. A dual exponential

functions fits the auto-correlogram curve with time constants of 1.7 and 33 s, decaying to a baseline value of $r = 0.56$.

3.5. Reactivation of firing rate modulations

Fig. 4A shows the correlation present in a recorded pyramidal cell population between the *maze* modulation variable X_{MS1} and the *sleep 2* modulation variable X_{S2S1}. The two variables were very strongly correlated (*reactivation correlation*; $r^2 = 0.56$, $p < 10^{-6}$). No correlation was found when the role of *sleep 1* and *sleep 2* were switched (preactivation control): Fig. 4B shows the correlation between the *maze* modulation variable (with respect to *sleep 2*), X_{MS2} and the *sleep 1* modulation variable, X_{S1S2} (*control preactivation*; $r^2 = 0.012$, $p > 0.55$). The effect is consistent and is observed in all three experiments, with the reactivation correlation larger than the control correlation in a large majority of experimental sessions (Fig. 4C–F), 11 out of 13 sessions for Experiment A, 13 out of 16 sessions in Experiment B, 22 out of 27 sessions for the Maze 1 phase of Experiment C, 22 out of 27 sessions for the Maze 2 phase of Experiment C).

3.6. Firing rate reactivation is stronger during sharp waves

Some features of firing rate reactivation resemble closely what was observed for the reactivation of cell-pair correlations. Kudrimoti et al. (1999) showed that the reactivation of zero-lag cell-pair correlations was stronger during sharp wave events
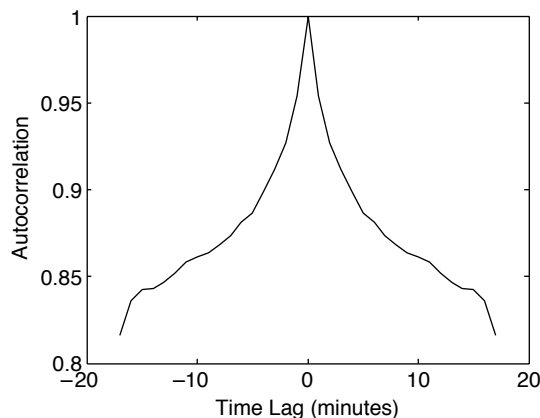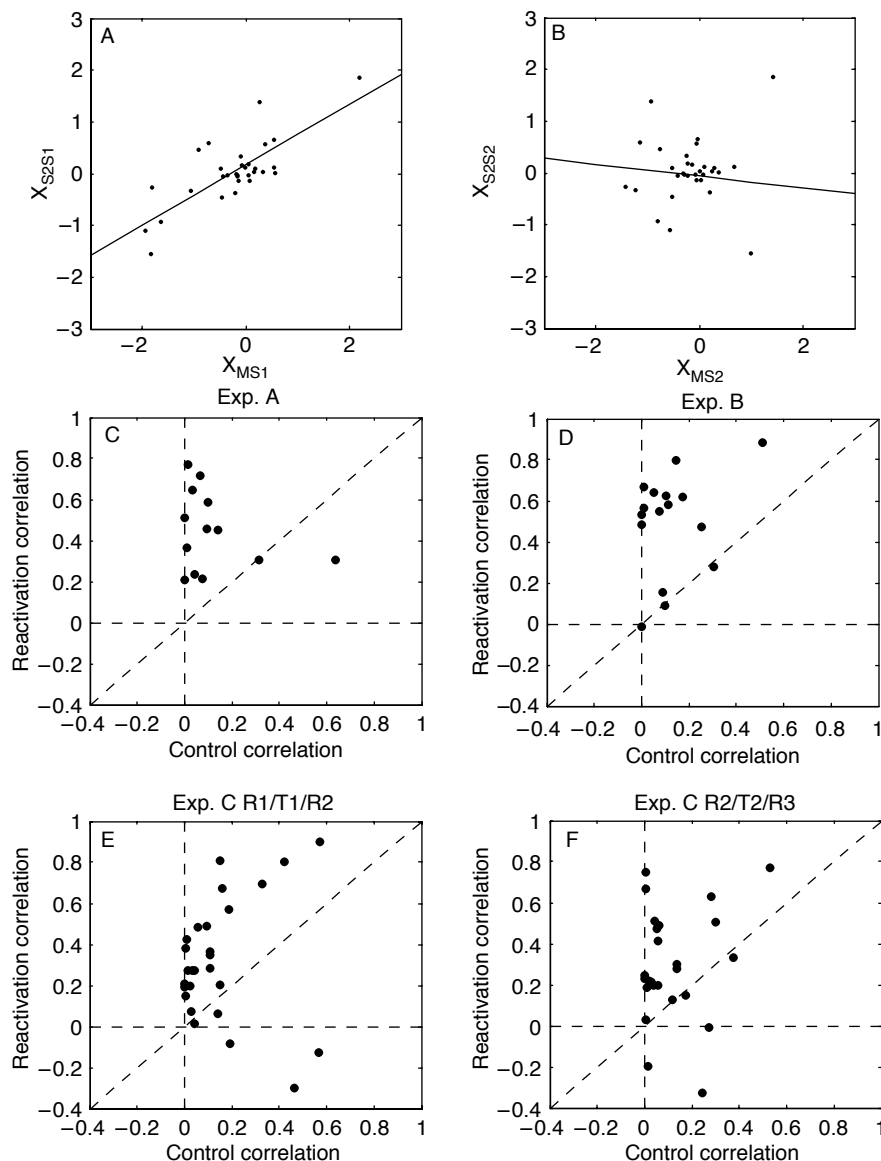

Fig. 3. Population vector auto-correlogram. The correlation between population vectors (computed in 1 min time bins) averaged over all the pairs of population vectors at a fixed time lags are plotted as a function of the time lag.

Fig. 4. Reactivation of firing rate modulations. A. Example of the correlation between the log-firing rate modulation X_{MS1}, modulation of the log-firing rate during the *maze* epoch with respect to the *sleep 1* epoch (X-axis), and the log-firing rate modulation X_{S2S1} of the *sleep 2* epoch with respect to the *sleep 1* epoch (*reactivation* correlation). The data from one session of Experiment A with 26 pyramidal cells are shown (each point corresponds to a pyramidal cell). B. Example of the *control* correlation from the same dataset as in A. In the control correlation, the role of the *sleep 1* and *sleep 2* epochs are switched. C–F. Comparison of the reactivation and the control correlation for all the experimental sessions in Experiment A (C), in Experiment B (D), for the two *maze* epochs in Experiment C (E and F). Each data point corresponds to an experimental session.

than in the inter-sharp wave periods. Fig. 5 shows that firing rate reactivation follows a similar pattern. For all three experiments the reactivation correlation was stronger during sharp waves than in inter-sharp waves periods. Interestingly, the control preactivation correlation was higher in the inter-sharp wave periods.

3.7. Time course of firing rate reactivation

Kudrimoti et al. (1999) also showed that cell-pair correlation reactivation decreased during the 20 min of the post-experience sleep session. Similarly, a downward trend is

observed for all three experiments analyzed here, as shown in Fig. 6, most clearly for Experiment C.

3.8. Correlation between firing rate reactivation and cell-pair correlation reactivation in some experimental conditions

Sleep reactivation fluctuates substantially across experimental sessions, because it reflects features of the ongoing brain dynamics on which the experimenter has very little control.

If firing rate reactivation and the correlation measures of reactivation are both indices of the same underlying
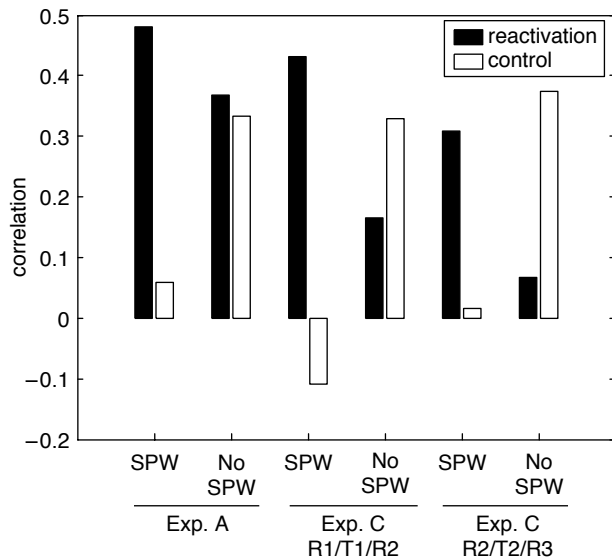
Fig. 5. Reactivation of firing rate modulations during sharp waves and non-sharp waves periods. Average reactivation (*black* bars) and control (*white* bars) correlation across sessions for the three experiments. Sleep log-firing rates measured during Sharp-Wave Events (*SPW*) and during the inter-sharp wave periods (*No SPW*).

physiological phenomena, it is plausible that these two measures will covary across experimental sessions. This was the case in two experimental conditions: for the 'cue-poor' track in Experiment A (Fig. 7A) and for one of the two rats in Experiment B (Fig. 7B), where a correlation significant at the $p < 0.05$ was observed between the reactivation correlation and the explained variance measure of cell-pair correlation. No correlation was observed in the other cases.

3.9. Modeling reactivation induced by synaptic plasticity and by excitability changes

Firing rate modulations and cell-pair correlations are two different characterizations of ensemble activity, both showing experience-induced reactivation, and as seen above, possibly related to each other. The theory of attractor networks suggests a simple theoretical scenario in which the reactivation of these two measures indeed arise as a consequence of the same

mechanisms. As shown by Shen and McNaughton (1996), experience-dependent plasticity acting on the synapses of a recurrent network can induce reactivation in simulated spontaneous activity. During experience, plasticity will act on a synaptic matrix that is already formed, and that may already encode attractor configurations. The activity during the maze session may reflect configurations that are already encoded by the synaptic matrix (Kesner and Rolls, 2001; Samsonovich and McNaughton, 1997). Those attractors most active during the maze session may then be tagged, so that they correspond, in a neural network analogy, to deeper energy minima, and would therefore occur more often during subsequent spontaneous activity. The more frequent appearance of those configurations would increase both the firing rate of the cells participating in the attractor and the correlation between them, thus generating the reactivation both of firing rate modulations and of cell-pair correlations. These possibilities were investigated with the help of simulations of a recurrent network of threshold-linear neurons.

Fig. 8 shows, as demonstrated by Amit and Brunel (1997) and by van Vreeswijk and Sompolinsky (1998), that randomness in the synaptic matrix is sufficient to generate the variability in baseline average firing rates across cell populations. In the simulations, the cells in pattern ξ^l were tagged as active during behavior. Fig. 9 shows the effect of synaptic modifications strengthening that pattern: The average overlap between the pattern ξ^l and the spontaneous activity configurations increases as a function of the synaptic potentiation parameter α (Fig. 9A).

Consequently, the firing rate of the cells participating in ξ^l increases with α, whereas the average firing rate of the other cells stays unmodified (Fig. 9B), and the correlation between those cells increases as well (Fig. 9C). This shows that synaptic plasticity may cause reactivation both of correlations and of firing rate modulations. Conversely, experience may induce activity-dependent changes in cell excitability. Simulations show that, in the model, this is enough to tag that attractor so that it will present itself more often during spontaneous activity (Fig. 10A), that the cell participating in the attractor are more spontaneously active (Fig. 10B), and that cell-pair correlation between cells in the attractor are increased as well (Fig. 10C).
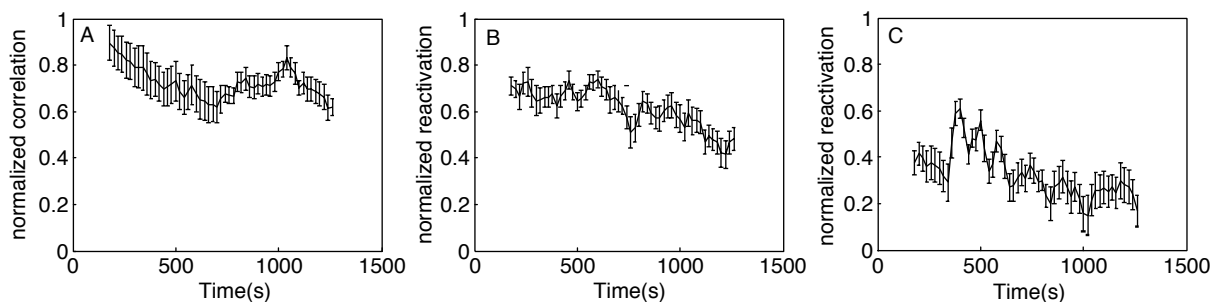

Fig. 6. Time course of firing rate modulation reactivation during the *sleep 2* epoch. The normalized reactivation correlation (for each datasets the correlation was normalized so that the maximum across time bin was 1) is plotted for the firing rates measured in 1 min time bins during the *sleep 2* epoch (the firing rates from the full *sleep 1* and *maze* epochs were used). Data for Experiment A (A), B (B), and C (C) are shown. *Error bars*: 95% bootstrap confidence interval.
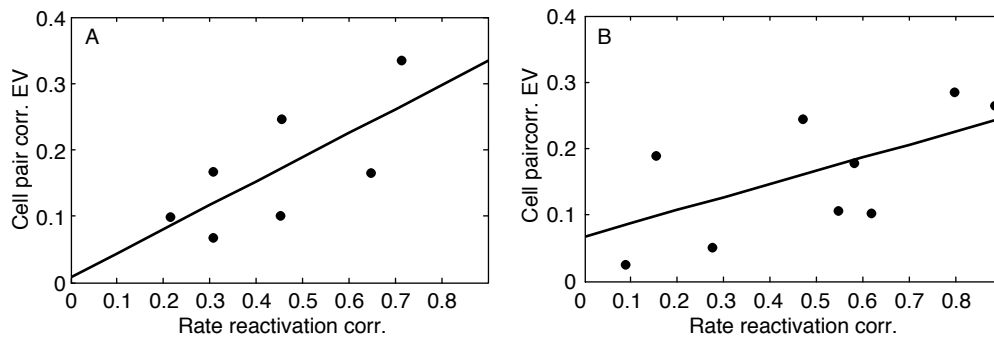
Fig. 7. Across-experimental sessions comparison of firing rate modulation reactivation (reactivation correlation *X*-axis) and cell-pair correlation (EV measure *Y*-axis). A. Sessions of Experiment A (*cue-rich* track). B. Sessions of Experiment B.

4. Discussion

We investigated the dynamics of pyramidal cell firing rates in rats during a *sleep–maze–sleep* paradigm. We found that (1) firing rates are highly correlated across all sessions; (2) cell populations that increase firing rate over baseline during maze running also reactivate during later sleep; (3) The correlation of maze and post-behavior sleep firing rates was strongest during sharp waves, and decayed with time since maze running, over a timescale of approximately 20 min.

A variety of experimental and statistical approaches have previously been applied to the question of reactivation. In early work, Pavlides and Winson (1989), recording from cell pairs, found that neurons for which the rat was physically constrained to the place field fired at elevated rates in subsequent sleep. Subsequently, Wilson and McNaughton (1994) showed that neuronal pairs showing elevated correlations during behavior continued to exhibit them in subsequent sleep (see also Kudrimoti et al., 1999). Other studies have investigated reactivation of the temporal order of neuronal pairs or spike sequences (Lee and Wilson, 2002; Louie and Wilson, 2001; Nadasdy, Hirase, Czurko, Csicsvari, & Buzsaki, 1999; Skaggs and McNaughton, 1996). Firing rates were investigated in more detail by Hirase, Leinekugel, Czurko, Csicsvari, and Buzsaki
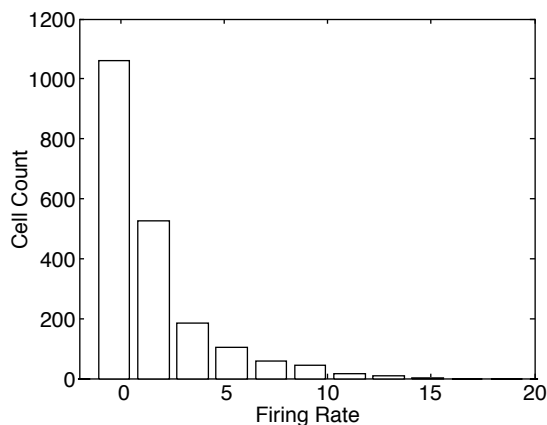

Fig. 8. Average population log-firing rate in the simulated spontaneous activity. The average is performed across the stable configurations reached when the network dynamics relaxed in the presence of external noise; 500 different noise realizations were considered. The data refer to the baseline condition (no synaptic or excitability changes).

(2001), showing a difference in correlation structure between familiar and novel environments.

This body of work, accumulated over a decade, together constitutes a strong case for memory-trace reactivation; however, the precise nature of the reactivation process remains unclear, at both the single cell and assembly levels. Reactivation is likely a complex and highly variable process, requiring novel statistical approaches. In this paper, we have seen some of the analytic complications that can arise, even when only looking at mean firing rates.

This difficulty arises in part from the nature of the statistical paradigm. In the traditional Neyman-Pearson approach, inferences are made by refutation of a null hypothesis. The primary difficulty is not in satisfactorily refuting a null hypothesis, but rather in precisely stating a null hypothesis of no reactivation, that does not require unjustified assumptions. Even in the simple firing rate framework considered here, assumptions are required, such as the lack of correlation between sleep sessions 1a and 1b. One can also conceive of ways the null hypothesis may be violated without *bona fide* memory-trace reactivation, such as an imbalance in the number of sharp waves amongst sleep sessions. Furthermore, other technical concerns may arise, such as electrode drift (although in our case this would only lead to a Type I error if it occurred precisely between the *sleep 1* and *maze* epochs) or spike-sorting errors (Quirk and Wilson, 1999), which are known to be especially severe during sharp waves (Harris, Henze, Csicsvari, Hirase, & Buzsaki, 2000). These concerns are to some extent ameliorated by the reduction in reactivation seen after swapping pre- and post-behavior sleep sessions ('preactivation'). Preactivation might indicate neural processes reflecting genuine anticipation: while reactivation was strongest during sharp wave events, preactivation was strongest in inter-sharp wave periods, suggesting that reactivation might occur during sleep and/or inactive behavior, whereas preactivation might be associated with epochs of greater activity. Alternatively, preactivation could be an indication of statistical issues requiring further clarification, even in the simple case of firing rates. We suspect that these concerns apply also to more complex analyses that have investigated synchrony patterns and temporal sequences.

Interestingly, some details of our results mirror the results of correlation and sequence-based analyses. In particular, we
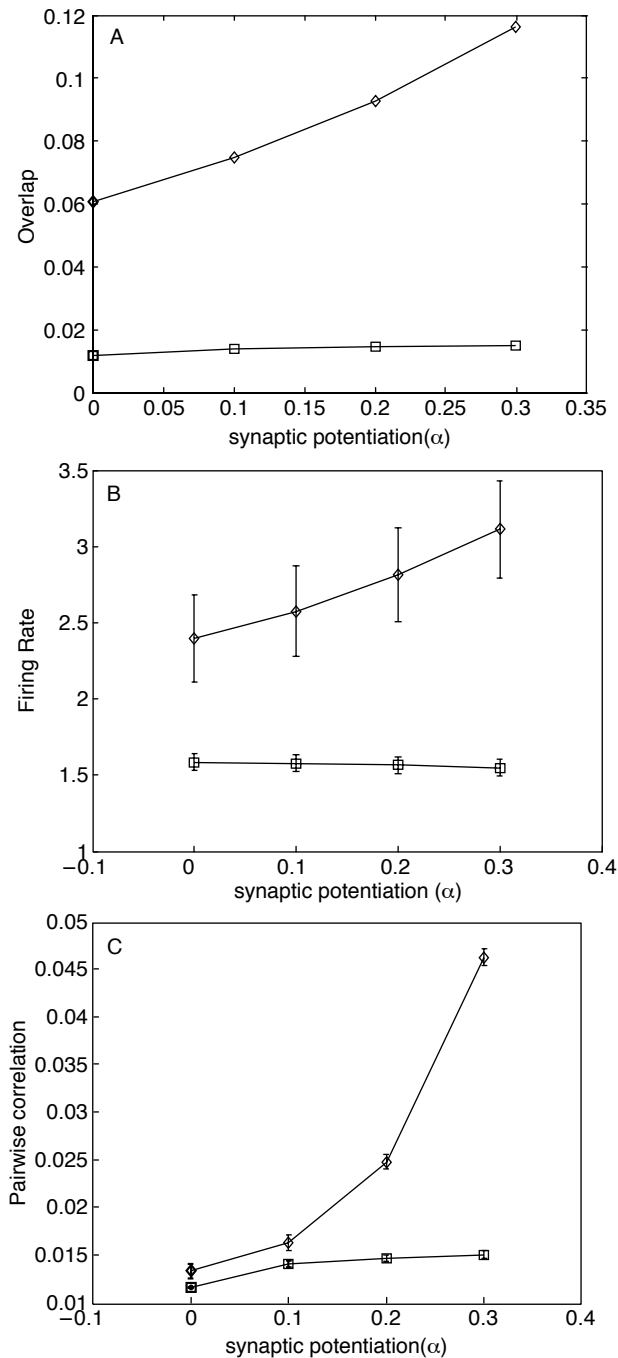
Fig. 9. Effect of synaptic potentiation on the network spontaneous activity. The following variables are plotted as a function of the synaptic potentiation level: A. The average overlap between the stable-state configurations and the tagged pattern (*diamonds*) and non-tagged patterns (*squares*). B. The average firing rate for units in the tagged pattern (*diamonds*) and the other units (*squares*). C. The average correlation between cell pairs in the tagged patterns (*diamonds*) and between cells pairs in the other patterns (*squares*).
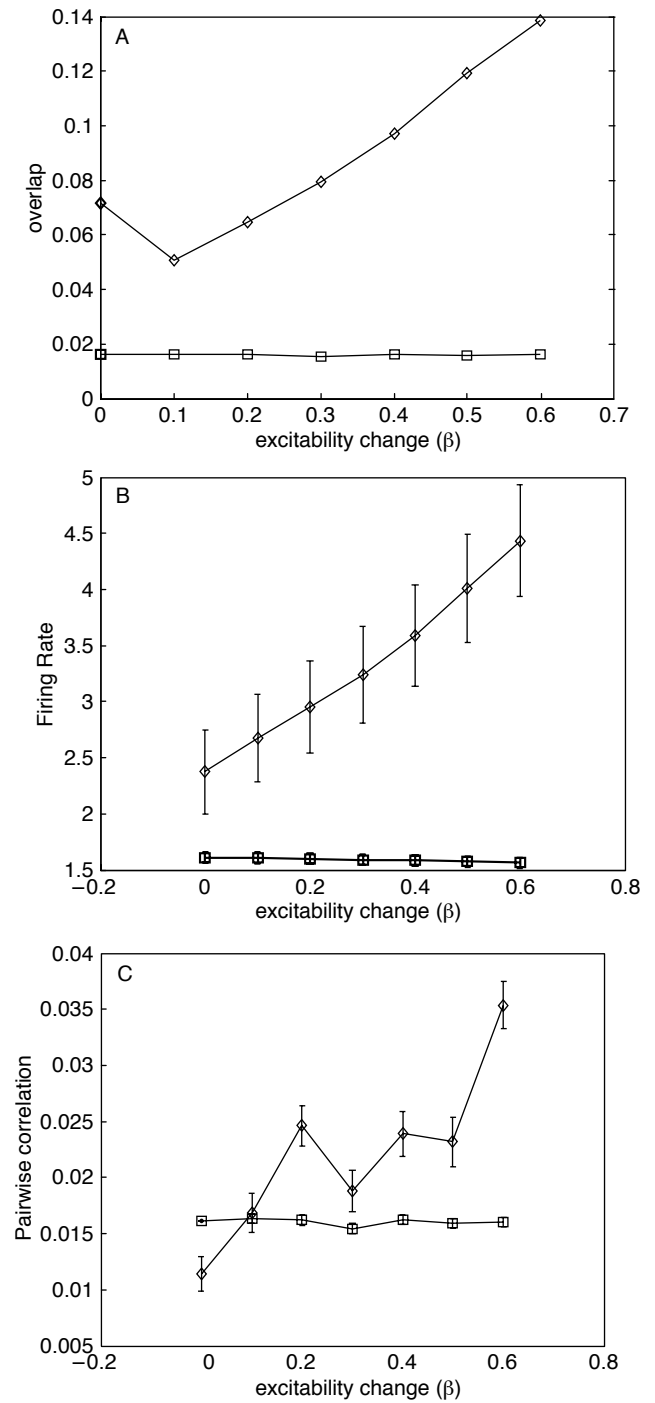
Fig. 10. Effect of changes in excitability on the network spontaneous activity. The following variables are plotted as a function of the synaptic potentiation level: A. The average overlap between the stable-state configurations and the tagged pattern (*diamonds*) and non-tagged patterns (*squares*). B. The average firing rate for units in the tagged pattern (*diamonds*) and the other units (*squares*). C. The average correlation between cell pairs in the tagged patterns (*diamonds*) and between cells pairs in the other patterns (*squares*).

observe a similar time course (reactivation decays during a 20 min period following behavior), and see more reactivation during sharp waves. Furthermore, we find that sessions showing higher rate reactivation also show higher cross-correlation reactivation.

Apart from this phenomenological similarity we do not, at present, have definitive arguments demonstrating that all the

measures of reactivation considered here are manifestations of the same underlying phenomenon. Recently, reactivation of cross-correlations has been found in some experimental conditions to depend on NMDA receptor functionality (Stanis et al., 2004), suggesting it may be at least partly caused by

synaptic plasticity. In principle at least, firing rate reactivation may originate from simpler processes, for example from experience dependent changes in neuronal excitability (Zhang and Linden, 2003). Processes of this kind, while probably important in many kinds of learning, are unlikely to be able to store and process a large amount of information, of the order of magnitude required by spatial/episodic memory in the hippocampus. At most, they may provide a total information storage capacity of the order of N bits, where N is the number of neurons. On the other hand, the storable information in the synaptic matrix with a Hopfield like rule is of the order of the number of synapses (probably about three orders of magnitude larger than the number of neurons in the hippocampus; (Amit, 1989; Battaglia and Treves, 1998; Treves, 1990).

A possible unifying framework may be found in the cell assembly concept and the theory of attractor networks. In our simple simulation, the role of experience is only to *select* one (or more) of some pre-wired attractors, in analogy to what proposed as a model for working memory in the absence of synaptic plasticity by Kesner and Rolls (2001). The attractor is, in essence, the cell assembly proposed by Hebb (Amit, 1994; Harris, 2005; Hebb, 1949; McNaughton and Morris, 1987) as the indivisible unit of brain function. It is also, in our view, the indivisible unit of reactivation and consolidation processes. Several different microscopic processes, at the cellular and/or synaptic level, might shape these assemblies or to prime pre-wired assemblies so that they will be more likely to activate in later spontaneous activity. In the model explored here, both Hebbian synaptic plasticity and experience dependent spike facilitation could successfully prime the cell assemblies elicited by experience. The reactivation of those cell assemblies reproduced both the firing rates and the correlation structure observed during experience, so that in this case firing rate and correlation measures are indeed indices of the same phenomenon.

A rate model, such as that used here, cannot reproduce the fine details of the temporal dynamics or the precise structure of cross-correlations (see e.g. Shen and McNaughton, 1996), for which a spiking neuron model is probably necessary. On the other hand, this simple simulation protocol addresses the issue of how the network responds to random noise, as a possible model of spontaneous activity, by analyzing the set of fixed-point activity configurations reached by the network in the presence of each realization of an uncorrelated, uniform random noise. In particular, the synaptic structure of the network will introduce correlations in the neuronal responses to the uncorrelated noise input and those correlations can be seen as a model of at least some plasticity related aspects of the measured experimental cross-correlations (Goldberg, Rokni, & Sompolinsky, 2004; Shen and McNaughton, 1996).

In reality, synaptic plasticity, spike facilitation and other microscopic phenomena may intervene differentially in different conditions, so that rate and correlation measures may actually not be perfectly correlated, as it was observed here under some conditions. We hope that the study of the interaction between cellular mechanisms and cell assembly reactivation can take advantage of statistical tools such as those proposed here.

References

Amit, D. J. (1989). *Modeling brain function*. Cambridge, UK: Cambridge University Press.

Amit, D. J. (1994). The hebbian paradigm reintegrated: Local reverberations as internal representations. *Behavioral and Brain Sciences*, *18*, 617–626.

Amit, D. J., & Brunel, N. (1997). Dynamics of a recurrent network of spiking neurons before and following learning. *Network*, *8*, 373–404.

Battaglia, F. P., Sutherland, G. R., & McNaughton, B. L. (2004). Local sensory cues and place cell directionality: Additional evidence of prospective coding in the hippocampus. *The Journal of Neuroscience*, *24*, 4541–4550.

Battaglia, F. P., & Treves, A. (1998). Attractor neural networks storing multiple space representations: A model for hippocampal place fields. *Physical Review E*, *58*, 7738–7753.

Broadbent, N. J., Squire, L. R., & Clark, R. E. (2004). Spatial memory, recognition memory, and the hippocampus. *Proceedings of the National Academy of Sciences, USA*, *101*, 14515–14520.

Buzsaki, G. (1989). Two-stage model of memory trace formation: A role for "noisy" brain states. *Neuroscience*, *31*, 551–570.

Buzsaki, G. (2004). Large-scale recording of neuronal ensembles. *Nature Neuroscience*, *7*, 446–451.

Goldberg, J. A., Rokni, U., & Sompolinsky, H. (2004). Patterns of ongoing activity and the functional architecture of the primary visual cortex. *Neuron*, *42*, 489–500.

Gothard, K. M., Skaggs, W. E., Moore, K. M., & McNaughton, B. L. (1996). Binding of hippocampal CA 1 neural activity to multiple reference frames in a landmark-based navigation task. *The Journal of Neuroscience*, *16*, 823–835.

Harris, K. D. (2005). Neural signatures of cell assembly organization. *Nature Reviews Neuroscience*, *6*, 399–407.

Harris, K. D., Henze, D. A., Csicsvari, J., Hirase, H., & Buzsaki, G. (2000). Accuracy of tetrode spike separation as determined by simultaneous intracellular and extracellular measurements. *The Journal of Neurophysiology*, *84*, 401–414.

Hebb, D. O. (1949). *The organization of behavior*. New York, NY: Wiley and Sons.

Hirase, H., Leinekugel, X., Czurko, A., Csicsvari, J., & Buzsaki, G. (2001). Firing rates of hippocampal neurons are preserved during subsequent sleep episodes and modified by novel awake experience. *Proceedings of the National Academy of Sciences, USA*, *98*, 9386–9390.

Hoffman, K. L., & McNaughton, B. L. (2002). Coordinated reactivation of distributed memory traces in primate neocortex. *Science*, *297*, 2070–2073.

Karten, Y.J., Cowen, S.L., Lindstedt, E.R., Kudrimoti, H.S., Gerrard, J.L., McNaughton, B.L., & Barnes, C.A. (2002). Reactivation of activity of neural ensembles during sleep in the rat hippocampus is not affected by positive or negative events during waking. Program No. 678.9. 2002 Abstract Viewer/Itinerary Planner. Washington, DC: Society for Neuroscience, Online.

Kesner, R. P., & Rolls, E. T. (2001). Role of long-term synaptic modification in short-term memory. *Hippocampus*, *11*, 240–250.

Kudrimoti, H. S., Barnes, C. A., & McNaughton, B. L. (1999). Reactivation of hippocampal cell assemblies: Effects of behavioral state, experience, and EEG dynamics. *The Journal of Neuroscience*, *19*, 4090–4101.

Lee, A. K., & Wilson, M. A. (2002). Memory of sequential experience in the hippocampus during slow wave sleep. *Neuron*, *36*, 1183–1194.

Louie, K., & Wilson, M. A. (2001). Temporally structured replay of awake hippocampal ensemble activity during rapid eye movement sleep. *Neuron*, *29*, 145–156.

Marr, D. (1970). A theory for cerebral neocortex. *Proceedings of the Royal Society London B: Biological Sciences*, *176*, 161–234.

Marr, D. (1971). Simple memory: A theory for archicortex. *Philosophical Transactions of the Royal Society London B: Biological Sciences*, *262*, 23–81.

McNaughton, B. L., Barnes, C. A., Battaglia, F. P., Bower, M. R., Cowen, S. L., Ekstrom, A. D., et al. (2003). Off-line reprocessing of recent memory and its role in memory consolidation: A progress report. In P. Maquet, C. Smith, & B. Stickgold (Eds.), *Sleep and brain plasticity* (pp. 225–246). Oxford, UK: Oxford University Press.

McNaughton, B. L., & Morris, R. G. M. (1987). Hippocampal synaptic enhancement and information storage within a distributed memory system. *Trends in Neurosciences*, *10*, 408–415.

Moser, E., Moser, M. B., & Andersen, P. (1993). Spatial learning impairment parallels the magnitude of dorsal hippocampal lesions, is hardly present following ventral lesions. *The Journal of Neuroscience*, *13*, 3916–3925.

Nadasdy, Z., Hirase, H., Czurko, A., Csicsvari, J., & Buzsaki, G. (1999). Replay and time compression of recurring spike sequences in the hippocampus. *The Journal of Neuroscience*, *19*, 9497–9507.

Pavlides, C., & Winson, J. (1989). Influences of hippocampal place cell firing in the awake state on the activity of these cells during subsequent sleep episodes. *The Journal of Neuroscience*, *9*, 2907–2918.

Pennartz, C. M., Lee, E., Verheul, J., Lipa, P., Barnes, C. A., & McNaughton, B. L. (2004). The ventral striatum in off-line processing: ensemble reactivation during sleep and modulation by hippocampal ripples. *The Journal of Neuroscience*, *24*, 6446–6456.

Quirk, M. C., & Wilson, M. A. (1999). Interaction between spike waveform classification and temporal sequence detection. *Journal of Neuroscience Methods*, *94*, 41–52.

Redish, A. D., & Touretzky, D. S. (1998). The role of the hippocampus in solving the morris water maze. *Neural Computation*, *10*, 73–111.

Riedel, G., Micheau, J., Lam, A. G. M., Roloff, E. v. L., Martin, S. J., Bridge, H., et al. (1999). Reversible neural inactivation reveals hippocampal participation in several memory processes. *Nature Neuroscience*, *2*, 898–905.

Rolls, E. T., & Treves, A. (1998). *Neural networks and brain function*. Oxford, UK: Oxford University Press.

Samsonovich, A., & McNaughton, B. L. (1997). Path integration and cognitive mapping in a continuous attractor neural network model. *The Journal of Neuroscience*, *17*, 5900–5920.

Shen, B., & McNaughton, B. L. (1996). Modeling the spontaneous reactivation of experience-specific hippocampal cell assembles during sleep. *Hippocampus*, *6*, 685–692.

Skaggs, W. E., & McNaughton, B. L. (1996). Replay of neuronal firing sequences in rat hippocampus during sleep following spatial experience. *Science*, *271*, 1870–1873.

Stanis, J.J., Dees, J.A., Gerrard, J.L., Lipa, P., VanRhoads, S.R., McNaughton, B.L., & Barnes, C.A. (2004). Reactivation of hippocampal neural ensemble patterns is NMDA receptor-dependent Program No. 329.20. 2004 Abstract Viewer/Itinerary Planner. Washington, DC: Society for Neuroscience, Online.

Sutherland, G. R., & McNaughton, B. (2000). Memory trace reactivation in hippocampal and neocortical neuronal ensembles. *Current Opinion in Neurobiology*, *10*, 180–186.

Treves, A. (1990). Graded-response neurons and information encodings in autoassociative memories. *Physical Review A*, *42*, 2418–2430.

van Vreeswijk, C., & Sompolinsky, H. (1998). Chaotic balanced state in a model of cortical circuits. *Neural Computation*, *10*, 1321–1371.

Wilson, H. R., & Cowan, J. D. (1972). Excitatory and inhibitory interactions in localized populations of model neurons. *Biophysical Journal*, *12*, 1–24.

Wilson, M. A., & McNaughton, B. L. (1993). Dynamics of the hippocampal ensemble code for space. *Science*, *261*, 1055–1058.

Wilson, M. A., & McNaughton, B. L. (1994). Reactivation of hippocampal ensemble memories during sleep. *Science*, *265*, 676–679.

Zhang, W., & Linden, D. J. (2003). The other side of the engram: Experience-driven changes in neuronal intrinsic excitability. *Nature Reviews Neuroscience*, *4*, 885–900.